Timing performance of Cherenkov-radiator-integrated MCP-PMT

Timing Performance of Cherenkov-Radiator-Integrated MCP-PMT

Rsyoke Ota, Kyohei Nakajima, Izumi Ogawa, Yoichi Tamagawa, Hideki Shimoi, Motohiro Suyama, and Tomoyuki Hasegawa

***Abstract*–Coincidence time resolution (CTR) of 10 ps is an ultimate goal toward reconstruction-less positron emission tomography (PET). One of the ways to enhance the timing performance of the PET detector is to make use of Cherenkov photons which is promptly emitted on the order of picosecond. A Cherenkov detector composed of a Cherenkov radiator and a fast photo-detector, such as a microchannel plate photomultiplier tube (MCP-PMT) can reach the CTR better than 100 ps full width at half maximum (FWHM). Previously, we have developed the Cherenkov detector where the Cherenkov radiator is integrated with the MCP-PMT to enhance the timing performance, and the CTR of 41.9 ps FWHM was obtained. In this study, we performed two types of experiments; (1) increasing statistics roughly ten times larger than the previous study to precisely determine the timing performance of the detector, (2) stepping a ^{22}Na point source and validating transitions of timing histograms according to the source positions. As a result, the CTR of 41.7 ps FWHM was obtained. Moreover, the CTR between the radiator and the MCP direct interaction was also investigated and approximately 55 ps FWHM was obtained. The transitions of the timing histograms according to the source positions were successfully observed. Finally, we show physical components affecting the CTR and potential capability toward the ultimate goal of 10 ps CTR is discussed.**

I. Introduction

Coincidence time resolution (CTR) is one of parameters which represent performance of a time-of-flight positron emission tomography (TOF-PET). Signal to noise ratio (SNR) of images obtained by the TOF-PET is highly affected by the CTR. Recently, a PET scanner with CTR of 210 ps has been released from Siemens, and the SNR of the PET images has been successfully improved [1]. The CTR of 210 ps is equivalent to position resolution of 31.5 mm along a line of response (LOR) between a pair of detectors. As the position resolution of 31.5 mm is worse than the spatial resolution, image reconstruction processes, which tend to amplify the noise in the images and are typically time consuming, are required. If the CTR could approach to 10 ps, the position resolution could be 1.5 mm, which is better than the spatial resolution of clinical PET scanners [2], and annihilation positions can be directly and three-dimensionally localized on an event-by-event basis. In this case, the image reconstruction process can be removed, and high SNR PET images would be obtained with lower dose or shorter scan times. Thus, it is worthwhile to develop a PET detector with the CTR of 10 ps.

One of the ways to enhance the timing performance of the PET detector is to make use of Cherenkov photons which are promptly emitted on the order of picosecond [3,4]. A PET detector composed of a Cherenkov radiator (Lead fluoride, PbF_2) and a fast photo-detector (microchannel plate photomultiplier tube, MCP-PMT) has been developed, and the CTR of 71 ps full width at half maximum (FWHM) has been achieved more than eight years before (2011) [5]. The PbF_2 crystal is suitable for the Cherenkov radiator because it has high refractive index (n = 1.82) and high transparency toward ultra violet region (cutoff = 245 to 280 nm) [6,7]. However, the high refractive index causes large optical mismatch between the radiator and the window face plate (WFP) of the MCP-PMT. The large optical mismatch reduces light collection efficiency of the detector, that would worsen both timing performance and detection efficiency for the radiations. Therefore, the optical boundary should be removed from the detector.

In 2018, we have developed a Cherenkov-radiator-integrated MCP-PMT (CRI), where the WFP of the ordinary MCP-PMT was replaced with the Cherenkov radiator and an Al_2O_3 intermediate layer was fabricated between the radiator and the photocathode using atomic layer deposition technique [8]. The optical boundary was successfully removed and a pair of the CRIs showed the CTR of 41.9 ps FWHM. However, the CTR measurement was performed under a condition where an ^{22}Na point source is fixed. In addition, the statistics should be increased to precisely determine its timing performance.

In this study, we perform two types of experiments; (1) increasing the statistics roughly ten times larger than the ref. [8] to precisely determine the timing performance the the CRI, (2) stepping the source position and validating transitions of timing histograms according to the source positions. Finally, we discuss future improvement of the detector toward 10 ps CTR.

II. Materials and Methods

Fig. 1 shows the experimental setup for increasing the statistics. The pair of CRIs were located face-to-face 200 mm away from each other. The entrance surfaces of the CRIs were

Manuscript received Dec. 10 2019.

Ryosuke Ota is with the Central Research Laboratory, Hamamatsu Photonics K. K., Hamamatsu, Japan (telephone: +81-53-586-7111, e-mail: Ryosuke.ota@crl.hpk.co.jp), and is also with the Graduate school of engineering, University of Fukui, Fukui, Japan.

Kyohei Nakajima, Izumi Ogawa, and Yoichi Tamagawa are with the Faculty of engineering, University of Fukui, Fukui, Japan.

Hediki Shimoi is with the Electron Tube Division, Hamamatsu Photonics K. K., Iwata, Japan.

Motohiro Suyama is with the Global Strategic Challenge Center, Hamamatsu Photonics K. K., Hamamatsu, Japan.

Tomoyuki Hasegawa is with the School of Allied Health Science, Kitasato University, Kitasato, Japan.

978-1-7281-4164-0/19/$31.00 ©2019 IEEE

covered by a black tape (Super 33+, 3M) to suppress reflections of the Cherenkov photons in the radiator. The ^{22}Na point source with a 1 mm ϕ lead collimator with 50 mm thickness was put at the center of the CRIs. The anode signals were directly fed into an oscilloscope (DSO-404A, Keysight) with a set bandwidth of 4.2 GHz at 20 GS/s to digitize the waveforms. The total measurement time is roughly ten times longer than the previous experiment of ref. [8].

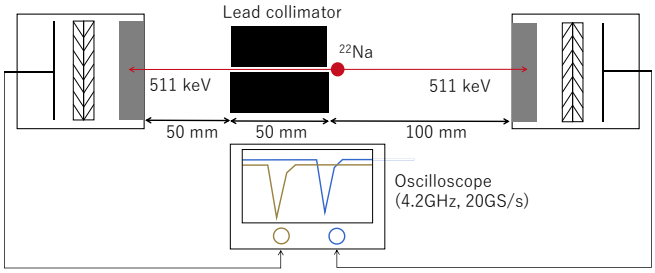

Fig. 1. Experimental setup for increasing the statistics. The ^{22}Na point source was put at the center of the CRIs. The anode signals from the detector were directly fed into an oscilloscope to digitize the waveforms.

Fig. 2 illustrates the experimental setup for stepping the source positions. Note that the lead collimator is not illustrated for visibility in the figure 2, but the point source was, in fact, attached to the lead collimator. The collimator and the point source were on an X-stage (TSD-604S, SIGMAKOKI) mounted on a carrier (CAA-60LS, SIGMAKOKI). The point source was stepped in intervals of 1.5 mm, and data for 9 different source positions were totally acquired. As the interval of 1.5 mm is equivalent to the time difference of 10 ps, the interval of the peak positions of the timing histograms would be 10 ps.

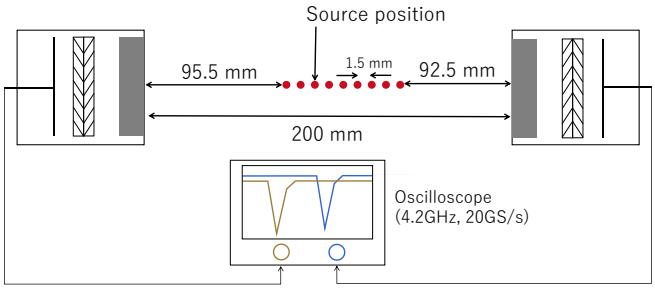

Fig. 2. Experimental setup for stepping the source position. Note that the lead collimator is not illustrated in this figure for visibility, but the point source was, in fact, attached to the lead collimator. The lead collimator and the point source were on an X-stage mounted on a carrier. The point source was stepped in intervals of 1.5 mm. Totally, data for 9 different source positions were acquired.

Flow of data analysis is the same as the ref. [8] and [9]. The acquired data were analyzed using ROOT [10]. A spline curve was obtained from the waveform data on an event-by-event basis using TSpline3 class method in ROOT. Detection timing of each detector at 5% for the pulse height was numerically calculated and the time difference between the CRIs were measured. The number of 5% showed the best CTR.

III. Results

A. Increasing statistics

The histograms of time difference between the CRIs with a fitting function of "4 Gaussians + Constant" is depicted in fig. 3. The 4 Gaussians are for the center peak, the two side peaks, and a broadened distribution below the main peak, that is caused by photoelectrons backscattering on the surface of the MCP. The "constant" is for accidental coincidence events. The center peak showed the CTR of 41.7 ps FWHM, while the two side peaks showed the CTR of 53.7 and 56.1 ps FWHM, respectively. The center peak is well represented by the single Gaussian even though the center peak contains two types of interactions; coincidence between the radiator and radiator and between the MCP and MCP. Estimating that the CTR of MCP-MCP events is worse than that of the radiator-radiator event, the CTR of the center peak could be improved if the lead-free MCP based CRI is developed.

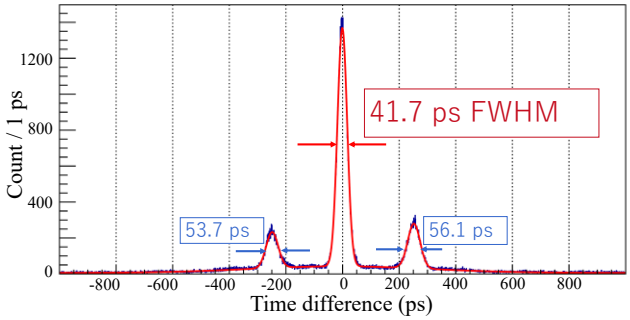

Fig. 3. Histogram of time difference between the CRIs. The histogram was fitted by the function of "4 Gaussians + Constant". The center peak showed the CTR of 41.7 ps FWHM, while the two side peaks showed the CTR of 53.7 and 56.1 ps FWHM.

B. Stepping source position

Histograms with 9 different source positions can be seen in fig. 4. The peak position is shifted according to the source position. For each source positions, the CTR does not differ from each other. Relationship between the known source positions and the measured peak positions with a linear fitting is illustrated in fig. 5. The linear relationship could be obtained. The slope of the relationship was 6.70 ± 0.07 ps/mm. Moreover, residual between the known source positions and the source positions estimated from the measured peak positions could be calculated. As a result, the position resolution is approximately validated as 0.2-0.3 mm. As the size of the point source is 0.25 mm, this result is reasonable.

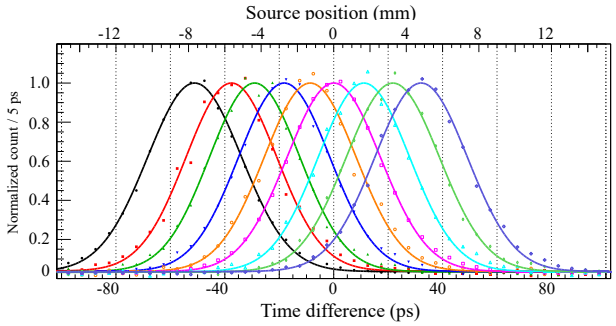

Fig. 4. Histograms with 9 different source positions. The peak position is shifted according to the source position.

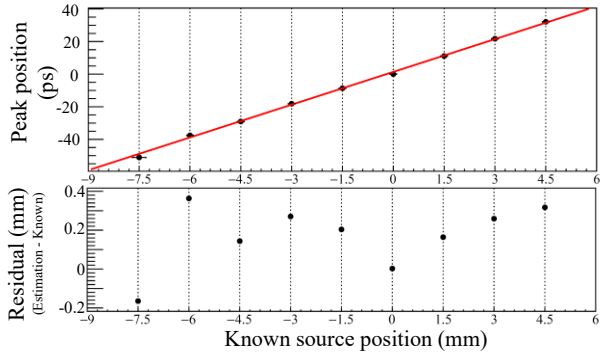

Fig. 5. Top: Relationship between the known source positions and the measured peak positions with a linear fitting. The slope was 6.70 ± 0.07 mm/ps. Bottom: residual between the known source positions and source positions estimated from the measured peak positions.

IV. Discussion

The CTR of the pair of CRIs were validated as 41.7 ps FWHM by increasing the statistics. The CTR of 41.7 ps could be deconvolved into 4 types of physical components as can be seen in fig. 6. Currently, the main factor contributing the CTR would be single photon time resolution (SPTR) of the CRI, and it is 25 ps FWHM for each detector. The second factor would be the photon travelling time spread in the radiator, and it was simulated as 17 ps FWHM [11]. The remained components would be the electric noise and the mixing of the radiator-radiator and MCP-MCP events. The factor of the mixing can be estimated as 10 ps considering the shape of the histogram described in fig. 3 [12].

To achieve 10 ps CTR, all factors should be improved. Simply, the factor of the mixing σ_{Mixing} would be removed by using the lead free MCP. The factor of the electric noise σ_{Noize} would be removed by carefully performing the baseline correction. The factor of the photon travelling time spread σ_{Photon} would be corrected by depth of interaction (DOI) information. We have already investigated feasibility of obtaining the DOI information from the Cherenkov detector using principal component analysis or deep learning technique [11, 13], and the DOI resolution would be 1-2 mm. As this number is smaller than the thickness of the radiator in the CRI, the σ_{Photon} could be improved. At last, to reduce the factor of the SPTR σ_{SPTR}, there are two approaches. One is simply to improve the SPTR of the CRI, and another one is to increase the number of Cherenkov photons by developing and optimizing the radiator. In the current CRI, the average number of detected Cherenkov photons might be only one. For example, if the number of Cherenkov photons increased up to 10, the σ_{SPTR} could be down to $25/\sqrt{10} = 7.9$ ps. Thus, the development of the optimal radiator allows us to approach the ultimate goal of 10 ps CTR.

$$CTR = \sqrt{2\sigma^2_{\mathrm{SPTR}} + \sigma^2_{\mathrm{Photon}} + \sigma^2_{\mathrm{Noise}} + \sigma^2_{\mathrm{Mixing}}}$$

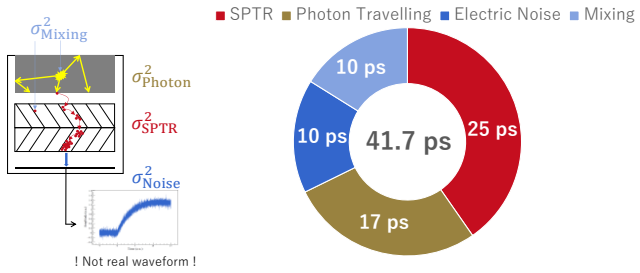

Fig. 6. Factors affecting the CTR in the CRI. Currently, the most contributing component to the CTR is the single photon time resolution (SPTR) of the CRI. Hence, improvement of the SPTR itself and development of an optimal Cherenkov radiator is necessary.

V. Conclusion

In this study, we performed the two types of experiments. The CTR of the pair of the CRIs was 41.7 ps FWHM while the CTRs of the two side peaks were 53.7 and 56.1 ps FWHM, respectively. The peak positions of the histograms of the time difference between the CRIs were successfully shifted according to the source positions. To achieve the CTR of 10 ps, the CRI based on the lead-free MCP, DOI capability, and optimization of the Cherenkov radiator are indispensable.

References

[1] J. van Sluis, et al., "Performance Characteristics of the Digital Biograph Vision PET/CT System," J. Nucl. Med., vol. 60, pp. 1031-1036, 2019.

[2] S. Vandenberghe, et al., "Recent developments in time-of-flight PET," EJNMMI Phys., vol. 3, 2016.

[3] P. Lecoq, et al., "Factors influencing time resolution of scintillators and ways to improve them," Trans. Nucl. Sci., vol. 57, pp. 2411-2416, 2010.

[4] S. Gundacker, et al., "Measurement of intrinsic rise times for various L(Y)SO and LuAG scintillators with a general study of prompt photons to achieve 10 ps in TOF-PET," Phys. Med. Biol., vol 61, pp. 2802-2837, 2016.

[5] S. Korpar, et al., "Study of TOF PET using Cherenkov light," Nucl. Instrum. Method A, vol. 654, pp. 532-538, 2011.

[6] D. F. Anderson, et al., "Lead fluoride: an ultra-compact Cherenkov radiator for EM calorimetry," Nucl. Instrum. Method A, vol. 290, pp. 385-389, 1990.

[7] M Miyata, et al., "Development of TOF-PET using Cherenkov radiation," J. Nucl. Sci. Tech., vol. 43, pp. 339-343.

[8] R. Ota, et al., "Coincidence time resolution of 30 ps FWHM using a pair of Cherenkov-radiator-integrated MCP-PMTs," Phys. Med. Biol., vol. 64, pp. 07LT01, 2019.

[9] R. Ota, et al., "Timing performance evaluation Cherenkov-based radiation detectors," Nucl. Instrum. Method A, vol. 924, pp. 1-4, 2019.

[10] R. Brun and F. Rademakers, "," Nucl. Instrum. Method A, vol. 389, pp. 81-86, 1997.

[11] R. Ota, et al., “Cherenkov radiation-based three-dimensional position-sensitive PET detector: A Monte Carlo study,” Med. Phys., vol. 45, pp. 1999-2008, 2018.
[12] R. Ota, et al., Precise analysis of timing performance of Cherenkov-radiator-integrated MCP-PMT: Analytical deconvolution of MCP direct interaction,” will be submitted.
[13] F. Hashimoto, et al., “A feasibility study on 3D interaction position estimation using deep neural network in Cherenkov-based detector: a Monte Carlo simulation study,” Biomed. Phys. Eng. Express., vol. 5, pp. 035001, 2019.